

Gravitational radiation timescales for extreme mass ratio inspirals

Jonathan R. Gair

Institute of Astronomy, Madingley Road, Cambridge, CB3 0HA, UK

Daniel J. Kennefick

*Theoretical Astrophysics, California Institute of Technology, Pasadena, CA 91125, USA
and Department of Physics, University of Arkansas, Fayetteville, AR 72701, USA*

Shane L. Larson

*Center for Gravitational Wave Physics, The Pennsylvania State University, University
Park, PA 16802, USA*

ABSTRACT

The capture and inspiral of compact stellar objects into massive black holes is an important source of low-frequency gravitational waves (with frequencies $\sim 1 - 100\text{mHz}$), such as those that might be detected by the planned Laser Interferometer Space Antenna (LISA). Simulations of stellar clusters designed to study this problem typically rely on simple treatments of the black hole encounter which neglect some important features of orbits around black holes, such as the minimum radii of stable, non-plunging orbits. Incorporating an accurate representation of the orbital dynamics near a black hole has been avoided due to the large computational overhead. This paper provides new, more accurate, expressions for the energy and angular momentum lost by a compact object during a parabolic encounter with a non-spinning black hole, and the subsequent inspiral lifetime. These results improve on the Keplerian expressions which are now commonly used and will allow efficient computational simulations to be performed that account for the relativistic nature of the spacetime around the central black hole in the system.

Subject headings: Stellar captures – loss cone – gravitational radiation – inspirals

1. Introduction

The event rate for detection of extreme mass ratio inspirals (EMRIs) with LISA depends on the efficiency of capture of compact objects by massive black holes in galactic

nuclei. Current event rate estimates (Gair et al. 2004) are derived using results from stellar dynamics simulations of nuclear star clusters (Hils & Bender 1995; Sigurdsson & Rees 1997; Freitag 2001; Freitag & Benz 2002; Ivanov 2002; Freitag 2003; Hopman & Alexander 2005), in which the clusters are dynamically evolved over the lifetime of a galaxy. Of central importance to these simulations is the estimate of the effect of gravitational radiation on the evolution of a particle’s orbital parameters as a function of proximity to the central black hole. The comparison of gravitational radiation timescales against cluster interaction timescales is a way to quantify whether a star stays bound to the black hole (eventually spiralling in to its death) or if it returns to the parent star cluster and is scattered away from the black hole by encounters with other stars. Scattering by other stars can also put the star onto a quasi-radial orbit so that it plunges into the black hole directly rather than inspiralling gradually. LISA will only be able to detect long lived inspirals (Gair et al. 2004), so it is important to quantify the fraction of captures that terminate in these two distinct ways. Simulations suggest that a significant fraction of captures will end in quasi-radial plunges rather than inspirals (Hils & Bender 1995; Hopman & Alexander 2005), which will impact the LISA event rate.

For any given encounter with the central black hole, the gravitational radiation inspiral lifetime τ_{gw} of a member of the population is compared against the two body relaxation timescale τ_{rlx} with other particles in the simulation. For an orbit of eccentricity e , if $\tau_{gw} < (1 - e) \tau_{rlx}$, the particle is removed from the simulation, and its orbital parameters are used to estimate the strength of the gravitational waves which might reach our detectors. If the relaxation timescale is such that $(1 - e) \tau_{rlx} < \tau_{gw}$, then two body encounters with other cluster members will alter the pericenter distance of a particle’s orbit before gravitational radiation reaction causes it to merge with the central black hole (Sigurdsson & Rees 1997; Ivanov 2002).

The conventional method for treating gravitational radiation in these simulations is to use the formalism of Peters and Mathews (Peters & Mathews 1963) and Peters (Peters 1964), which assumes the particles and central masses are point-like, Newtonian objects and that the particle orbits are Keplerian trajectories. This framework does not account for the fact that the central body is a black hole, and that the orbits and orbital evolution can be decidedly non-Keplerian in nature. This paper presents an improvement to the traditional Peters and Mathews treatment, based on perturbative calculations. By exploiting the extreme mass ratio of the system, the inspiralling object can be regarded as a small perturbation of the spacetime of the central black hole. While black hole perturbation theory is well understood (Poisson 2004), the solution requires extensive numerical calculations for general orbits. However, the orbits of interest in stellar dynamics calculations are usually highly eccentric, and for such orbits the inspiral timescale can be estimated to an accuracy

of $\sim 1\%$ (depending on the precise eccentricity at capture) simply by knowing the change in eccentricity during the first encounter with the black hole.

Data for the energy and angular momentum change on a parabolic orbit are available in the literature (Martel 2004), and can be used as a starting point for treating the dynamics of extreme mass ratio inspirals. Based on an understanding of the properties of geodesics in the Schwarzschild spacetime, it is possible to fit a simple function to this data; the corresponding formulae are all that is required by stellar dynamics codes and represent a significant improvement over the standard Keplerian treatment (Peters & Mathews 1963).

This paper is organised as follows. Section 2 describes geodesics in the Schwarzschild spacetime and provides fits for the total radiated energy ΔE and angular momentum ΔL on single parabolic encounters with the black hole. Section 3 presents an expression for the inspiral lifetime based on these fits. In Section 4 we briefly discuss how the gravitational radiation losses from orbits of arbitrary (low) eccentricity can be estimated and finally, Section 5 summarises the implications and possible applications of this work.

2. Geodesics and gravitational wave fluxes for parabolic orbits

The results of Peters and Mathews (Peters & Mathews 1963) for the radiated energy and angular momentum and the inspiral lifetime are simple to implement, with a low associated computational cost. This makes them ideal for use in large simulations. The formalism has the disadvantage that it treats the binary components as point masses on Keplerian orbits. Captured stars that evolve into an extreme mass ratio inspiral (EMRI) generally must pass very close to the black hole, where the orbit is very non-Keplerian. The Peters and Mathews treatment neglects important features of the gravitational wave emission due to the presence of the black hole.

One simple improvement that can be made is to use a “semi-relativistic” approximation, i.e., using the fully relativistic orbit in place of the Keplerian orbit, while using an approximation for the corresponding gravitational wave emission. This approach was first suggested by (Ruffini & Sasaki 1981) and is explored extensively in a companion paper (Gair et al. 2005). To compute things correctly, one must use black hole perturbation theory and solve the Teukolsky equation (Poisson 2004). The problem of radiation from orbits in the Schwarzschild spacetime was examined by (Cutler et al. 1994). They provided useful asymptotic results for nearly circular and nearly plunging orbits and tabulated fluxes for orbits with a variety of periapses and eccentricities. However, their code worked in the frequency domain, which is not well suited for dealing with the highly eccentric orbits of interest

in the capture problem. More recently, results for the fluxes of radiation from parabolic orbits in Schwarzschild have become available (Martel 2004), which were computed using a time domain code. Using insight gained from studying the geodesic equations (Gair et al. 2005), it is possible to derive a simple fitting function for the energy and angular momentum emitted that matches the perturbative results to within a fraction of a percent. This function may be implemented in stellar cluster simulations as easily as the Keplerian expressions and for little additional computational cost.

The Schwarzschild geodesic equations for an equatorial orbit (without loss of generality) are

$$\left(\frac{dr}{d\tau}\right)^2 = \left(\frac{E^2}{c^2} - c^2\right) + \frac{2GM}{r} \left(1 + \frac{L_z^2}{c^2 r^2}\right) - \frac{L_z^2}{r^2}, \quad (1)$$

$$\left(\frac{d\phi}{d\tau}\right) = \frac{L_z}{r^2}, \quad (2)$$

$$\left(\frac{dt}{d\tau}\right) = \frac{E}{(c^2 - 2GM/r)}, \quad (3)$$

where τ is the proper time along the geodesic, L_z is the conserved specific angular momentum of the particle¹, E is the conserved specific energy and M is the mass of the central black hole. In the weak field ($r \gg GM/c^2$ or $L_z \gg GM/c$), these reduce to the usual Keplerian equations of motion, the geodesic is a conic section and there is a well defined periapse and eccentricity. These are related to the orbital energy and angular momentum by

$$\frac{E}{c^2} = \sqrt{1 - \frac{GM(1 - e^K)}{c^2 r_p^K}}, \quad (4)$$

$$L_z = \sqrt{(1 + e^K) GM r_p^K}. \quad (5)$$

We have used “K” to denote a parameter defined in the Keplerian way. In the strong field, relativistic effects cause the orbit to deviate from Keplerian motion and the normal notion of eccentricity, as a geometrical parameter characterizing the shape of a conic section, is not valid. However, we can still define a relativistic orbital periapse, r_p^R , as the Schwarzschild radial coordinate of the inner turning point of the motion, and we can define a relativistic eccentricity, e^R , from r_p^R and the Schwarzschild coordinate of the outer turning point of the motion (the relativistic apapse, r_a^R), using the usual equation

$$e^R = \frac{r_a^R - r_p^R}{r_a^R + r_p^R}. \quad (6)$$

¹For equatorial orbits in Schwarzschild, the z-component of the angular momentum, $L_z = L$, the total angular momentum. We maintain the notation L_z in order to facilitate future comparisons with orbits in Kerr spacetimes, for which L_z is conserved, but not L .

The relationship between the relativistic parameters and the orbital energy and angular momentum is

$$\frac{E}{c^2} = \sqrt{1 - \frac{GM(1 - e^R)((1 + e^R)c^2 r_p^R - 4GM)}{c^2 r_p^R((1 + e^R)c^2 r_p^R - (3 + e^{R^2})GM)}}, \quad (7)$$

$$L_z = \frac{(1 + e^R)c\sqrt{GM}r_p^R}{\sqrt{(1 + e^R)c^2 r_p^R - (3 + e^{R^2})GM}}. \quad (8)$$

It is important to note the differences between (7)–(8) and (4)–(5). In simulations of stellar clusters the parameters of orbits that pass close to the black hole are generally computed using the Keplerian relations. However, this is not a good approximation for orbits that pass within a few Schwarzschild radii of the black hole. The energy and angular momentum are well defined out in the cluster where the orbital parameters are determined. Equating the right hand side of (7) with that of (4), and similarly for the right hand sides of (8) and (5), we can deduce a relationship between the Keplerian eccentricity and periaapse and the relativistic eccentricity and periaapse, for orbits which have a specified energy and angular momentum. We are mainly interested in highly eccentric orbits, so we work to linear order in $(1 - e^K)$.

$$\begin{aligned} r_p^R &= \frac{r_p^K}{2} \left(1 + \sqrt{1 - \frac{8GM}{c^2 r_p^K}} \right) \\ &\quad - \frac{(1 - e^K)}{2} \frac{GM}{c^2} \frac{\sqrt{r_p^K(r_p^K - 8GM/c^2)} + r_p^K - 8GM/c^2}{r_p^K - 8GM/c^2} \\ 1 - e^R &= \frac{(1 - e^K)}{2} \left(1 + \sqrt{1 - \frac{8GM}{c^2 r_p^K}} \right) \end{aligned} \quad (9)$$

The energy and angular momentum losses given below are expressed in terms of the relativistic (“R”) parameters, so it is important to use equation (9) to convert Newtonian parameters into their relativistic counterparts when evaluating gravitational wave fluxes. Indeed, even when using Peters and Mathews level approximations one should use the relativistic rather than the Keplerian parameters for better results. This approach was used in (Hopman & Alexander 2005) and we discuss it in more detail in Section 4.

For the rest of this section we will concentrate on parabolic orbits, i.e., orbits for which $e^K = e^R = 1$. A parabolic orbit has $E = c^2$ and is uniquely parameterised by its periaapse (or angular momentum). The angular momentum is related to the periaapse by

$$L_z = \frac{\sqrt{2GM} c r_p^R}{\sqrt{c^2 r_p^R - 2GM}}. \quad (10)$$

This should be compared to the Keplerian relation, $L_z = \sqrt{2GM r_p^K}$. The radial geodesic equation for a parabolic orbit is

$$\left(\frac{dr}{d\tau}\right)^2 = \frac{2GM}{r^3} (r - r_p^R) \left(r - \frac{2GM r_p^R}{c^2 r_p^R - 2GM}\right) \quad (11)$$

For any given eccentricity, there is a minimum value for the periaapse below which the orbit plunges directly into the black hole. This occurs when the two inner turning points of the geodesic equation coincide. For parabolic orbits this is $r_p^R = 4GM/c^2$. A geodesic with precisely this periaapse asymptotically approaches a circular orbit as it nears the periaapse, and spends an infinite amount of time whirling around the black hole. The asymptotic circular orbit is an unstable orbit of the gravitational potential. Cutler, Kennefick and Poisson (Cutler et al. 1994) call this orbit the ‘separatrix’, since it separates bound from plunging orbits in phase space.

In calculating the energy and angular momentum lost from an orbit, we must make the assumption of adiabaticity, i.e., that the timescale over which the parameters of the orbit change significantly due to gravitational radiation is much longer than the timescale of the orbit. This is valid in the extreme mass ratio limit, $m/M \ll 1$. Under this approximation, we treat the orbit as an exact geodesic of the spacetime, compute the corresponding radiation fluxes and then update the orbital parameters to a new geodesic before repeating this procedure. A particle on a separatrix orbit would radiate an infinite amount of gravitational radiation, as it spends an infinite time “whirling” around the black hole on a nearly circular orbit. In this case, adiabaticity breaks down and it is wrong to neglect the effect of radiation reaction. In practice a particle that starts on such an orbit would plunge into the black hole in a finite time. However, one still expects the energy and angular momentum losses to diverge as the separatrix is approached.

During the whirl phase, the orbit is almost circular, and so the total energy and angular momentum radiated will be approximately proportional to the number of “whirls” (i.e., complete revolutions in ϕ) that the orbit undergoes. Counting the number of whirls indicates that, for a parabolic orbit, the total radiated energy and angular momentum will diverge like the logarithm of $r_p^R - 4GM/c^2$ near the separatrix. The derivation of this result is given in more detail in (Gair et al. 2005), and was also discussed in (Cutler et al. 1994). For orbits that do not come near the black hole, the Keplerian approximation is expected to be valid. Therefore, in the limit $r_p^R \rightarrow \infty$, the energy and angular momentum radiated, ΔE and ΔL_z , should approach the Peters and Mathews results:

$$\Delta E = -\frac{85\pi}{12\sqrt{2}} c^2 \frac{m}{M} \left(\frac{c^2 r_p^R}{GM}\right)^{-\frac{7}{2}}, \quad \Delta L_z = -6\pi \frac{Gm}{c} \left(\frac{c^2 r_p^R}{GM}\right)^{-2}. \quad (12)$$

Our aim is to write a single expression for ΔE that can be used for any choice of r_p^R . Using the preceding arguments, we deduce that any such expression must diverge logarithmically near the separatrix at $r_p^R = 4GM/c^2$, and must recover (12) in the limit $r_p^R \rightarrow \infty$. Denoting $y = c^2 r_p^R/(GM)$, a functional form that has the correct behaviour in these two limits is

$$\begin{aligned} \frac{M}{m} \Delta X &= F_X(y) \\ &= \left(\sum_{n=0}^N A_n^X \left(\frac{(y-4)}{y^2} \right)^n \right) \cosh^{-1} \left[1 + B_0^X \left(\frac{4}{y} \right)^{N_X-1} \frac{1}{y-4} \right] \\ &\quad + \frac{(y-4)}{y^{1+\frac{N_X}{2}}} \sum_{n=0}^N C_n^X \left(\frac{(y-4)}{y^2} \right)^n + \frac{(y-4)}{y^{2+\frac{N_X}{2}}} \sum_{n=0}^{N-1} B_{n+1}^X \left(\frac{(y-4)}{y^2} \right)^n \end{aligned} \quad (13)$$

In this, X is either E/c^2 or $cL_z/(GM)$ and we fix $N_E = 7$, $N_{L_z} = 4$ to give the correct leading order behaviour (12) as $r_p^R \rightarrow \infty$. The parameter N gives the order of the fit, i.e., the number of terms in the expansion that we use. To ensure that the fitting function asymptotically approaches (12), we impose a constraint on the coefficient C_0^X

$$C_0^E = -\frac{85\pi}{12\sqrt{2}} - 64 A_0^E \sqrt{2 B_0^E}, \quad C_0^{L_z} = -6\pi - 8 A_0^{L_z} \sqrt{2 B_0^{L_z}} \quad (14)$$

Further discussion of this fitting function is given in (Gair et al. 2005). In that paper, we derive the fitting function coefficients that match the results of a “semi-relativistic” calculation. However, the most accurate calculation of energy and angular momentum fluxes requires solution of the Teukolsky equation. Data from such calculations is available in the literature for parabolic orbits around Schwarzschild black holes (Martel 2004). Using the data from that paper, we were able to derive fitting function coefficients to use in (13) that recover the Teukolsky results extremely well. In fact, taking $N = 2$ is sufficient for better than 0.2% accuracy, and the corresponding fit coefficients are

$$\begin{aligned} A_0^E &= -0.318434, & A_1^E &= -5.08198, & A_2^E &= -185.48, & B_0^E &= 0.458227, \\ B_1^E &= 1645.79, & B_2^E &= 8755.59, & C_0^E &= 3.77465, & C_1^E &= -1293.27, \\ C_2^E &= -2453.55, & A_0^{L_z} &= -2.53212, & A_1^{L_z} &= -37.6027, & A_2^{L_z} &= -1268.49, \\ B_0^{L_z} &= 0.671436, & B_1^{L_z} &= 1755.51, & B_2^{L_z} &= 9349.29, & C_0^{L_z} &= 4.62465, \\ C_1^{L_z} &= -1351.44, & C_2^{L_z} &= -2899.02 \end{aligned} \quad (15)$$

Figure 1 shows the percentage error in using this approximation over the range of periapse given by Martel. For comparison, we also show the error in using the Peters and Mathews result (12), evaluated for Keplerian and relativistic parameters. The error from using the fitting function (13) is significantly smaller than the difference between these fluxes and the

Peters and Mathews results. The fluctuations in the error are due to the difference between a smooth function and noisy numerical results. The magnitude of the difference is everywhere smaller than the numerical error that Martel quotes (1%) and is a factor of approximately 1000 smaller than the error using Peters and Mathews.

Expression (13) strictly applies only to parabolic orbits, i.e., with $e^R = 1$. In realistic situations, the eccentricity at capture will be very high, but less than unity, $0 < 1 - e_0^R \ll 1$. For such orbits, (13) can still be used and gives reliable results. The functional form fails if $r_p^R < 4GM/c^2$, but the last stable orbit (LSO) is related to the orbital eccentricity by $c^2 r_{p\ LSO}^R = 2GM(3 + e^R)/(1 + e^R)$ and so $r_{p\ LSO}^R > 4GM/c^2$ for all $e^R < 1$. In fact, for non-parabolic orbits, a slightly better expression for ΔE is obtained by using (13) with $(y - 4)$ replaced by $(y - 2(3 + e^R)/(1 + e^R))$ and $(4/y)$ replaced by $2(3 + e^R)/((1 + e^R)y)$ (there is some discussion of suitable fitting functions for generic orbits in (Gair et al. 2005)). However, for extremely eccentric orbits, this change only makes a difference for orbits that are extremely close to the LSO.

3. Inspiral Timescales

In stellar dynamics calculations which attempt to estimate the LISA EMRI event rate, one must determine when a given particle is captured by the central black hole. Broadly speaking, a particle is captured when $\tau_{gw} \lesssim (1 - e)\tau_{rlx}$ (as before, τ_{gw} and τ_{rlx} are the timescales for gravitational wave inspiral and two body relaxation respectively). Heuristically, the picture is that if the orbital parameters evolve rapidly enough due to the emission of gravitational radiation, the star will spiral into the black hole (be “captured”) before the cumulative perturbations to its orbit due to two-body encounters with other members of the cluster become large enough to put the star onto a new orbit which either does not come near the central black hole or plunges directly.

The canonical estimate of τ_{gw} is given by Peters (Peters 1964) for a star which initially has semi-major axis a_0 and eccentricity e_0 :

$$\tau_{gw} = - \int_0^{e_0^K} \frac{1}{de/dt} de = \frac{12c_0^4}{19\beta} \int_0^{e_0^K} de \frac{e^{29/19} [1 + (121/304)e^2]^{1181/2299}}{(1 - e^2)^{3/2}}, \quad (16)$$

where the constants c_0 and β are given by

$$c_0 = \frac{(r_p^K)_0(1 + e_0^K)}{e_0^{K12/19} [1 + (121/304)e_0^{K2}]^{870/2299}}, \quad \beta = \frac{G^3}{c^5} \frac{64}{5} M^2 m. \quad (17)$$

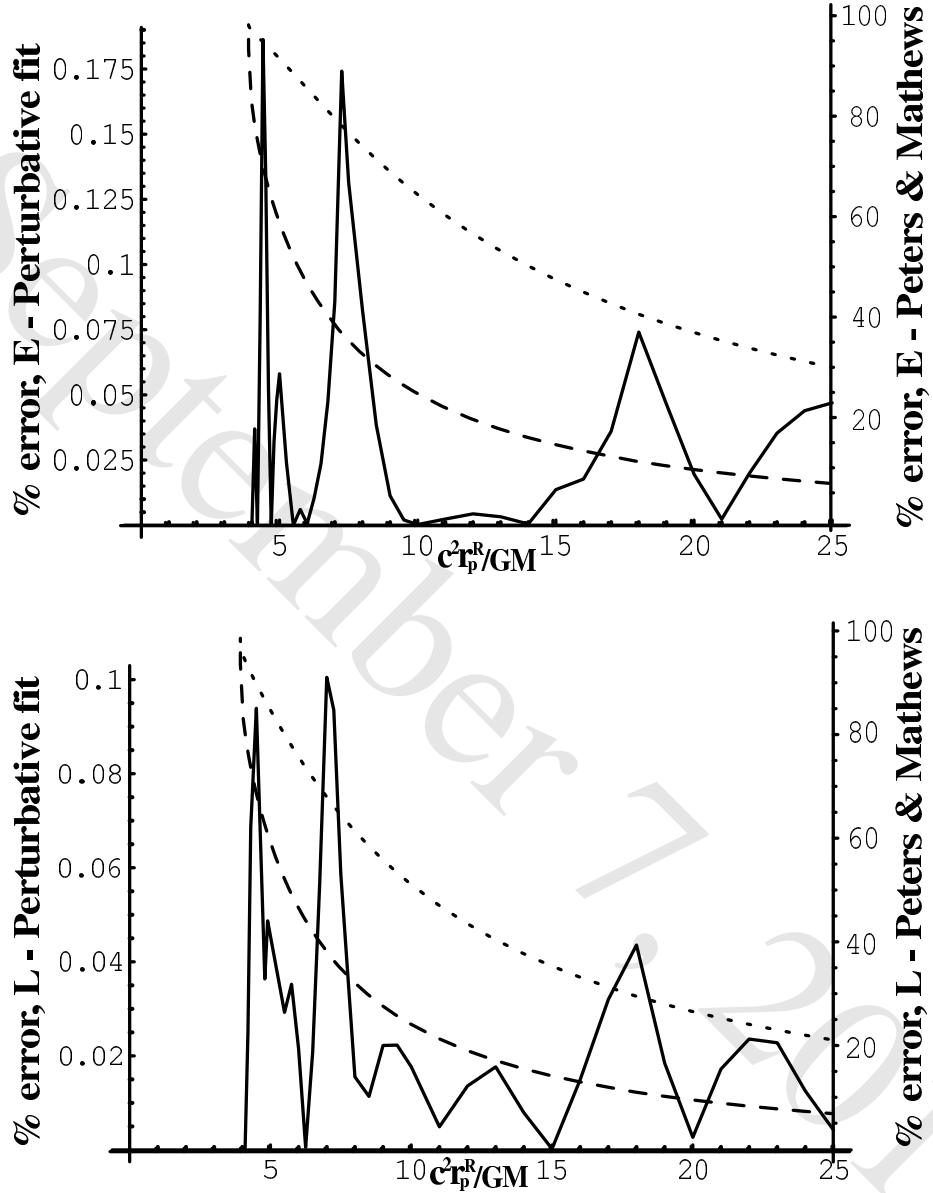


Fig. 1.— Accuracy of fit to relativistic fluxes – this figure shows the absolute percentage error when using the fitting function described in the text (solid line) to approximate the energy (upper) and angular momentum (lower) fluxes tabulated in Martel 2004. For comparison, we also show the error from using the Peters and Mathews result (12), evaluated for Keplerian (“K”) parameters (dotted line) and for relativistic (“R”) parameters (dashed line). Two different scales have been used – the left hand scale applies to the errors in the fitting function, while the right hand scale applies to the errors in both applications of Peters and Mathews. The horizontal axis is the value of the relativistic periastron, $c^2 r_p^R / GM$, of the geodesic in question.

In writing this and subsequent expressions in this section, we have assumed an extreme mass ratio, $M \gg m$ to set $M + m \approx M$.

Expression (16) is derived by integration of the Peters and Mathews fluxes over an inspiral. However, stars that become EMRI events for LISA are captured with very high eccentricity (typically $e \sim 0.9999$ or higher). In the limit $e_0^K \rightarrow 1$, expression (16) becomes (Peters 1964)

$$\tau_{gw}(r_p^K, e_0^K) \approx \frac{24\sqrt{2}}{85} \frac{c^5}{G^3 M^2 m} \frac{r_p^{K^4}}{\sqrt{1 - e_0^K}}. \quad (18)$$

This form of the timescale expression is used directly in some stellar cluster simulations (Hopman & Alexander 2005), and is a very accurate approximation to the true timescale for inspirals that are initially highly eccentric. The divergence of the inspiral timescale as $e_0^K \rightarrow 1$ arises from the divergence of the orbital timescale (at fixed periaapse) in the same limit

$$T_{orb}(r_p, e_0) \approx \frac{2\pi}{\sqrt{GM}} \left(\frac{r_p}{1 - e_0} \right)^{\frac{3}{2}}. \quad (19)$$

In equation (19) (and equations (20) and (21) below), r_p and e can be either the relativistic or the Keplerian values, so superscripts have been omitted. Equation (19) gives the dominant piece of the timescale even accounting for the presence of the black hole. For nearly parabolic orbits

$$\frac{de}{dt} \approx \frac{\Delta e(r_p, e = 1)}{T_{orb}(r_p, e)} \approx \frac{\sqrt{GM}}{2\pi} \left(\frac{1 - e}{r_p} \right)^{\frac{3}{2}} \Delta e(r_p, e = 1) \quad (20)$$

in which Δe is the change in eccentricity on a single orbit (the initial pass). The timescale for inspiral is dominated by

$$\tau_{gw}(r_p, e_0) \approx - \frac{2}{\Delta e(r_p, e = 1)} \frac{2\pi}{\sqrt{GM}} \frac{r_p^{\frac{3}{2}}}{\sqrt{1 - e_0}} \quad (21)$$

This expression is also given in (Hopman & Alexander 2005). In the Peters and Mathews approximation (Peters & Mathews 1963), $\Delta e^K(r_p^K, 1) = -85\pi (GM)^{3/2} Gm / (6\sqrt{2} c^5 r_p^{K^5/2})$, giving the result (18). Using the fits to the perturbative results, $\Delta e^R(r_p^R, e^R = 1)$ may be expressed

$$\begin{aligned} \Delta e^R(r_p^R, e^R = 1) &= \frac{\partial e^R}{\partial E} \Delta E(r_p^R, e^R = 1) + \frac{\partial e^R}{\partial L_z} \Delta L_z(r_p^R, e^R = 1) \\ &= 2 \frac{r_p^R}{GM} \Delta E(r_p^R, e^R = 1) \\ &= 2 \frac{c^2 r_p^R}{GM} \frac{m}{M} F_E \left(\frac{c^2 r_p^R}{GM} \right) \end{aligned} \quad (22)$$

where the function $F_E(y)$ is the fit to the energy loss derived earlier (13-15). Together, Eqs. (21) and (22) constitute an improved estimate of the inspiral lifetime.

Figure 2 compares the asymptotic timescale (21) computed using three methods – T_{asym}^{Pert} , generated using the perturbative result (22), T_{asym}^{KepPM} , generated using the Peters and Mathews result (18) evaluated for Keplerian (“K”) parameters and T_{asym}^{RelPM} , generated using the Peters and Mathews result (18) evaluated for relativistic (“R”) parameters. The figure shows the ratio of these various timescales as a function of the initial periapse of the orbit. This periapse is the *Keplerian* periapse of the orbit, which is the quantity normally evaluated in stellar cluster simulations. The Keplerian Peters and Mathews timescale is then given directly by (18), while the other timescales are given by first computing the corresponding relativistic periapse and eccentricity (9). The curves are actually eccentricity dependent, but curves for different eccentricities are almost indistinguishable for the eccentricities of interest, $10^{-2} \lesssim 1 - e^R \lesssim 10^{-6}$. The figure indicates that all three approximations agree for large initial periapses, but deviate as the periapse is reduced. Comparing to the standard Keplerian timescale, T_{asym}^{KepPM} , for $r_p^K \lesssim 80GM/c^2$, the perturbative timescale is smaller by 10% or more, while for $r_p^K \lesssim 16GM/c^2$, it is more than 50% lower. This is a reasonably large discrepancy, and it therefore seems plausible that inclusion of the more accurate decay timescale in stellar cluster simulations could enhance the capture rate. On a note of caution, a parabolic Keplerian orbit with periapse $r_p^K = 8GM/c^2$ corresponds to the relativistic orbit with periapse $r_p^R = 4GM/c^2$, i.e., the separatrix orbit. Thus, all orbits with Keplerian periapse less than $8GM/c^2$ are plunging orbits. The standard cut off used in most stellar cluster simulations is at a Keplerian periapse of $2GM/c^2$. This correction will thus tend to *decrease* the number of capture orbits. Whether this dominates over the enhanced rate due to the reduction in inspiral lifetime is not clear, but can be determined by simulation. This is currently being pursued.

It is also clear from Figure 2 that a significant part of the improvement derives from the coordinate choice, i.e., using the relativistic periapse and eccentricity (9). A significantly improved estimate of both the radiation fluxes and the inspiral timescale can be obtained simply by evaluating the standard Peters and Mathews results (12, 18) for the relativistically defined periapse and eccentricity (9). This is discussed briefly in Section 4 and in more detail in (Gair et al. 2005). Nonetheless, the perturbative timescale is still more than 20% shorter for $r_p^K \lesssim 16GM/c^2$, and should be used if possible. In (Hopman & Alexander 2005), relativistic parameters are used to describe the orbit and the cut off for plunging orbits is correctly defined. This might explain some of the reduction in event rate that they observe, although this reduction is dominated by diffusion onto plunging orbits. Inclusion of the perturbative results described here in the same type of simulation used in (Hopman & Alexander 2005) should lead to an enhancement in rate, but it is not entirely clear how large an effect this

will be.

An important point to note is that both expression (21) and the Peters expression (18) are derived by integrating the orbital averaged fluxes, $\langle de/dt \rangle$ and $\langle dr_p/dt \rangle$. In the test particle (zero mass) limit this is correct, but for non-zero mass ratios it will not be entirely accurate. The discrepancy is apparent from the fact that the gravitational decay timescale diverges like $(1 - e^R)^{-1/2}$ as $e^R \rightarrow 1$, which is less rapid than the divergence of the orbital period, $(1 - e^R)^{-3/2}$. If the particle was initially at periaapse, the decay timescale is not too inaccurate, but in practice the particle will start near apoapse, out in the stellar cluster. Physically, there are no significant gravitational radiation losses until the particle gets close to the black hole, so the decay timescale must be at least as long as half the first orbital period. The discreteness of the GW emission should become important when one minus the initial eccentricity of the orbit, $1 - e_0^R$, is less than the change in eccentricity on the first pass, $\Delta e^R(r_p^R, e^R = 1)$, i.e., when

$$(1 - e_0^R) \lesssim -2 \frac{m}{M} \frac{c^2 r_p^R}{GM} F_E \left(\frac{c^2 r_p^R}{GM} \right). \quad (23)$$

For this eccentricity, the change in $(1 - e^R)$ over the first orbit is of the same magnitude as $(1 - e_0^R)$, thus the underlying assumption that the particle completes an entire orbit on the initial geodesic is false. This is also the point at which the decay timescale (21) becomes comparable to the initial orbital period, so it is clear that the assumptions are breaking down. In this regime, the gravitational wave decay timescale is more accurately computed by assuming the periaapse and eccentricity change discretely at periaapse, and adding up the orbital periods of this sequence of geodesics. At the same level of approximation used to derive (21), the corresponding GW inspiral timescale is given by

$$\begin{aligned} \tau_{gw}(r_p^R, e_0^R) &\approx \frac{\pi}{\sqrt{GM}} \left(\frac{r_p^R}{1 - e_0^R} \right)^{\frac{3}{2}} + \frac{2\pi r_p^{R\frac{3}{2}}}{\sqrt{GM}} \sum_{l=1}^{\infty} \frac{1}{1 - e_0^R + l \Delta e^R(r_p^R, e^R = 1)} \\ &= \frac{\pi r_p^{R\frac{3}{2}}}{\sqrt{GM}} \left(\left(\frac{1}{1 - e_0^R} \right)^{\frac{3}{2}} + \left(\frac{1}{\Delta e^R(r_p^R, e^R = 1)} \right)^{\frac{3}{2}} \zeta \left(\frac{3}{2}, \frac{1 - e_0^R}{\Delta e^R(r_p^R, e^R = 1)} \right) \right) \end{aligned} \quad (24)$$

where $\zeta(z, q)$ is the generalised Riemann zeta function. The first term in (24) is the time taken to reach periaapse from apoapse on the first pass, while the second term is the summation of orbital periods over the subsequent sequence of geodesics. This expression neglects the change in periaapse on each pass, the difference in Δe^R on each pass due to the evolution of e^R and approximates a finite series (which terminates when $1 - e_0^R + l \Delta e^R$ equals the plunge eccentricity) with an infinite sum. However, these are all lower order corrections in the mass ratio, m/M , and may be neglected for initially highly eccentric extreme mass ratio inspirals.

In the limit $1 \gg 1 - e_0^R \gg \Delta e^R(r_p^R, e^R = 1)$, equation (24) is equivalent to (21), but when $1 - e_0 \approx \Delta e^R(r_p^R, e^R = 1)$, this is no longer true. Figure 3 shows the ratio of the integral timescale (21) to the discrete timescale (24) as a function of $(1 - e_0^R)/\Delta e^R(r_p^R, e^R = 1)$. As expected, the integral form (21) does well until the estimated point of breakdown (23), but significantly underestimates the decay timescale in the extreme parabolic limit. In this regime, a more accurate orbital decay timescale can be obtained by considering the sum of half the initial orbital period plus the decay time (21) evaluated for the orbit with periapse $r_p^{R'} = r_p^R + \delta r_p^R/2$ and eccentricity $e^{R'} = e^R + \delta e^R/2$, where δr_p^R and δe^R are the predicted change in periapse and eccentricity for the initial geodesic. In other words, we compute the integral decay timescale starting when the particle reaches periapse for the first time. This gives

$$\begin{aligned}
 \tau_{gw}(r_p^R, e_0^R) &= \frac{\pi}{\sqrt{GM}} \left(\frac{r_p^R}{1 - e_0^R} \right)^{\frac{3}{2}} - \frac{M}{m} \frac{2\pi\sqrt{GM}}{c^2 F_E \left(\frac{c^2 r_p^{R'}}{GM} \right)} \sqrt{\frac{r_p^{R'}}{1 - e^{R'}}} \\
 e^{R'} &= e^R + \frac{m}{M} \frac{c^2 r_p^R}{GM} F_E \left(\frac{c^2 r_p^R}{GM} \right) \\
 r_p^{R'} &= r_p^R + \frac{m}{M} \left(\frac{\sqrt{GM}(c^2 r_p^R - 2GM)^{\frac{3}{2}}}{\sqrt{2}c^2(c^2 r_p^R - 4GM)} F_{Lz} \left(\frac{c^2 r_p^R}{GM} \right) \right. \\
 &\quad \left. - \frac{(r_p^R)^2 c^2 (c^2 r_p^R - 2GM)}{2GM(c^2 r_p^R - 4GM)} F_E \left(\frac{c^2 r_p^R}{GM} \right) \right)
 \end{aligned} \tag{25}$$

Figure 3 also shows the ratio of the revised timescale (25) to the discrete timescale (24) (with the approximation $r_p^{R'} = r_p^R$). This expression performs very well in all regimes, and is at most a 2% overestimate near $1 - e_0 = \Delta e(r_p^R, e^R = 1)/4$. In most situations the difference between (21) and (25) is small, but for any initial eccentricity, there is a mass ratio where condition (23) holds, and in that regime (25) must be used. However, this expression is equally easy to evaluate in numerical codes.

4. Extension to generic orbits

This paper has focused on parabolic orbits, as these are of most relevance for astrophysical captures. For orbits of moderate eccentricity, this analysis will break down. If data based on perturbative calculations was available for the energy and angular momentum losses on generic orbits, it would be possible to compute a fit analogous to (13) that could be used generically (see discussion in (Gair et al. 2005)). This is not true at present. However, a significantly better approximation to the fluxes can be obtained simply by evaluating the

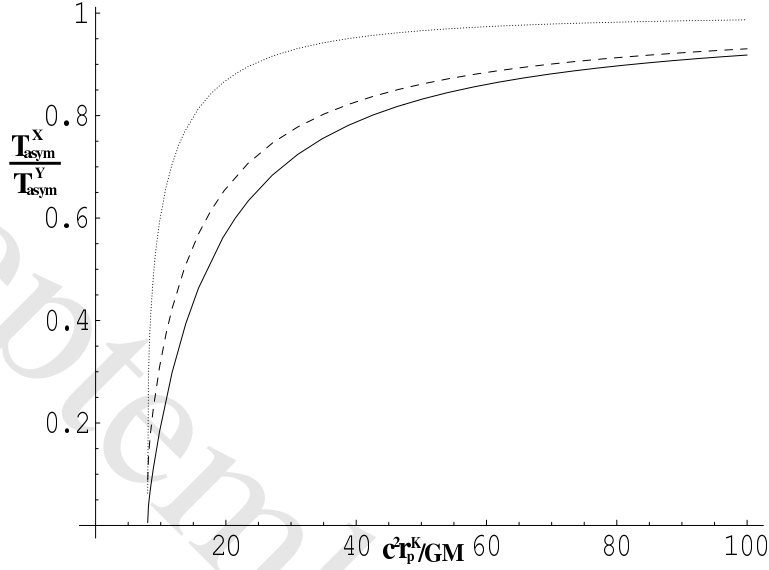


Fig. 2.— Comparison of the asymptotic approximation to the timescale (21) computed using the three methods described in the text. The plot shows the ratio $T_{asy}^{Pert}/T_{asy}^{KepPM}$ (solid line), the ratio $T_{asy}^{RelPM}/T_{asy}^{KepPM}$ (dashed line) and the ratio $T_{asy}^{Pert}/T_{asy}^{RelPM}$ (dotted line), as a function of the initial Keplerian periapse.

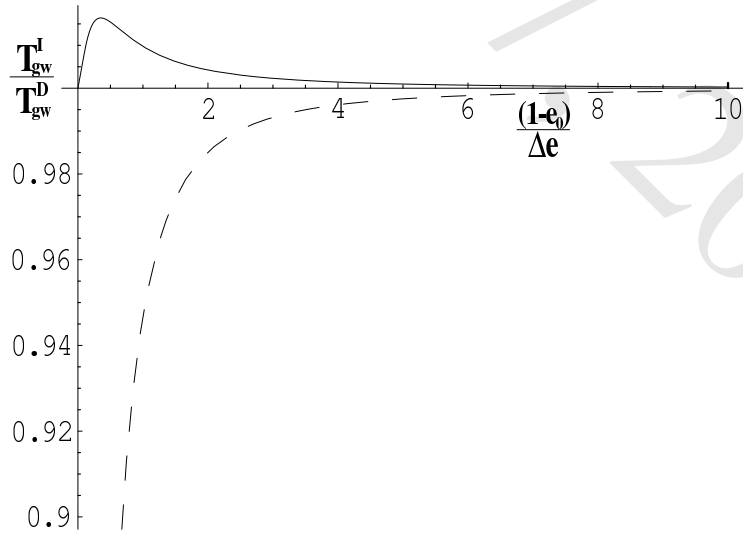


Fig. 3.— Ratio of the integral inspiral timescale (21), T_{gw}^I , to the discrete inspiral timescale (24), T_{gw}^D , as a function of $(1 - e_0^R)/\Delta e (r_p^R, e^R = 1)$. The dashed line uses the integral timescale computed directly from (21), while the solid line includes the first half period correction (25).

Peters and Mathews fluxes, using the relativistic (rather than the Keplerian) definition of the orbital parameters. This approach was used in (Hopman & Alexander 2005).

Inversion of equations (7)–(8) yields a quadratic to give e^R and r_p^R as functions of E and L_z (which can be obtained from the Keplerian parameters using (7)–(8) if necessary). For orbits of moderate eccentricity, $e \lesssim 0.9$, it is not appropriate to use the (eccentricity independent) flux expressions or timescale formula quoted earlier, since these were evaluated in the high eccentricity limit. However, if the relativistic eccentricity and periapse are computed for the orbit in question, a good approximation to the energy and angular momentum radiated can then be obtained using the Peters and Mathews expressions

$$dE = -\frac{64\pi c^2 m}{5} \frac{1}{M} \frac{1}{(1+e^R)^{\frac{7}{2}}} \left(1 + \frac{73}{24}(e^R)^2 + \frac{37}{96}(e^R)^4\right) \left(\frac{c^2 r_p^R}{GM}\right)^{-\frac{7}{2}} \quad (26)$$

$$dL_z = -\frac{64\pi Gm}{5} \frac{1}{c} \frac{1}{(1+e^R)^2} \left(1 + \frac{7}{8}(e^R)^2\right) \left(\frac{c^2 r_p^R}{GM}\right)^{-2}. \quad (27)$$

The corresponding inspiral timescale can be computed by integrating these fluxes along an inspiral trajectory, as in (16). We emphasise that for most situations of astrophysical interest in the capture problem, the parabolic results given earlier in this paper should be used. However, if fluxes for moderate eccentricity orbits are required, expressions (26-27) evaluated for the relativistic orbital parameters perform much better in the strong field than if they are evaluated for the Keplerian orbital parameters (Gair et al. 2005). That this approach will yield a better estimate of the energy and angular momentum fluxes is not clear a priori, but has been verified by comparing to fluxes computed using perturbation theory (Gair et al. 2005). This technique essentially identifies orbits that are geometrically similar. In the strong field, a Schwarzschild geodesic with a given energy and angular momentum is nothing like the Keplerian orbit with parameters (e^K, r_p^K) , but it does look somewhat like a Keplerian orbit with parameters (e^R, r_p^R) , e.g., the turning points of the motion are at the same radii etc. The orbital geometry is very important for determining the radiation field and this is probably the reason that a better estimate of the flux can be obtained via this procedure.

If more accurate fluxes are required for generic orbits, one can use the expressions quoted in (Barack & Cutler 2004). These are based on post-Newtonian expansions and are therefore only approximations to the true fluxes, but improve slightly on (26–27). For parabolic orbits, the fit presented here (13-15) gives the correct energy and angular momentum flux from an extreme mass ratio orbit under the assumption of adiabaticity. It is therefore more accurate than any post-Newtonian calculation for parabolic and highly eccentric orbits, and so should be used under those circumstances. Further flux expressions are given in

(Gair & Glampedakis 2005), which combine fits to perturbative calculations for the fluxes from circular orbits with post-Newtonian expressions for the fluxes from eccentric orbits. The resulting expressions improve on (Barack & Cutler 2004) and could be combined with (13-15) to interpolate the evolution of generic inspirals.

5. Discussion

In this paper, we have presented new simple analytic expressions for the energy and angular momentum radiated in gravitational waves by and subsequent inspiral lifetime of stars that pass close to black holes on nearly parabolic orbits. These expressions are based on the results of numerical perturbative calculations that are available in the literature (Martel 2004) and are considerably more accurate than the standard Keplerian results of (Peters & Mathews 1963) that are commonly used. We find that the inspiral lifetime can be significantly reduced when the capture problem is treated more carefully, which suggests an increase in the capture rate compared to the results of current simulations. However, the use of relativistic parameters for describing the orbit might actually lead to a reduction in events, since there are more plunging orbits.

Standard stellar cluster simulations (Freitag 2001; Freitag & Benz 2002; Freitag 2003) characterise capture as the point at which the gravitational wave inspiral timescale becomes comparable to the two body scattering timescale. Expression (25) can be easily implemented in this context in place of the usual Peters and Mathews timescale (16). More recently (Hopman & Alexander 2005) used Monte Carlo simulations to study the capture problem, but allowed for diffusion by two body scattering after gravitational wave emission had become important. They found that while the standard criterion, $\tau_{gw} = (1 - e) \tau_{rlx}$, is a reasonable approximation, there was a significant effect from scattering after this point, with many stars being perturbed onto plunge orbits rather than capture orbits. However, once $\tau_{gw} \lesssim 0.01(1 - e) \tau_{rlx}$, this effect was unimportant. At this point, the orbits are still in general extremely eccentric, and so the parabolic flux expressions (13-15) and inspiral timescale (21) are valid and improve significantly over Peters and Mathews. Thus, the improvements presented here could also be implemented easily in this type of diffusion calculation. In the future, we hope that the results in this paper will be usefully implemented in existing stellar cluster simulation codes to investigate what effect a more careful treatment of the gravitational radiation emission can have on capture rates.

The results presented here are strictly valid only for parabolic orbits, but perform well for any orbit with sufficiently high eccentricity ($e \gtrsim 0.9$). We expect that in the capture problem, all orbits of interest will be highly eccentric. However, there are other astrophysically

interesting scenarios in which inspiralling objects will begin on orbits with moderate or zero eccentricity. These include the formation of stars in an accretion disc around a black hole (Levin 2003; Goodman & Tan 2003), or the capture of stars by stripping of binaries in three body encounters (Miller et al. 2005). In section 4 we described a simple trick that can be used to improve the accuracy of the Peters and Mathews approximation to the gravitational radiation fluxes for orbits of moderate eccentricity. Simply by using a different parameterisation of the orbit and evaluating the usual flux expression for those parameters, significantly more accurate results can be obtained (Gair et al. 2005). The asymptotic approximation to the timescale (21) is no longer accurate when the initial eccentricity is moderate. However, capture is usually not the interesting question in astrophysical scenarios where this occurs, since the stars have already been brought onto close orbits by other mechanisms and so it will not usually be necessary to evaluate the capture criterion $\tau_{gw} < (1 - e) \tau_{rlx}$. If an inspiral timescale is required to determine the subsequent evolution, or parameter distribution of LISA sources, this may be computed by integrating the flux expressions along the inspiral trajectory. An important caveat is that the moderate eccentricity results quoted in Section 4 do not approach the parabolic results (13–15) in the limit $e \rightarrow 1$, except in the weak field, $r_p \rightarrow \infty$. This is simply because the parabolic results are based on accurate perturbative calculations, while the results in section 4 are approximations. For this reason, it would be unwise to combine both approaches in any single calculation. However, generally speaking the astrophysical situations in which the parabolic results are applicable are quite distinct from those in which the moderate eccentricity approximations are required. If it is necessary to follow an inspiral from capture right up to plunge, a scheme should interpolate appropriately between the parabolic expression (13–15) and either the moderate eccentricity expressions quoted in Section 4 or other schemes for evolving moderate eccentricity EMRIs (e.g., Barack & Cutler 2004, Gair & Glampedakis 2005).

The flux expressions (13–15) scale linearly with the mass ratio, m/M . This follows from the assumption of an extreme mass ratio, $m/M \ll 1$. As the mass ratio is increased, the approximations used here break down in various regimes. For highly eccentric orbits, the assumption that the gravitational wave emission can be averaged over the orbit no longer holds, and it is necessary to account for the fact that the emission occurs in short bursts near periapse. This was discussed at the end of section 3, and it can be accounted for in a reasonably simple way. A further consequence of increasing mass ratio is the failure of the adiabatic approximation. The energy and angular momentum fluxes are computed under the assumption that the source orbit is a geodesic of the spacetime. This is a reasonable assumption provided the timescale over which the orbital parameters change appreciably due to gravitational wave emission is long compared to the orbital timescale. This assumption breaks down if the mass ratio is too high or for orbits that lie close to the separatrix (for

which the energy and angular momentum losses diverge). Roughly speaking, the adiabatic approximation breaks down when the change in eccentricity/periapse on a single encounter with the black hole is a significant fraction of the orbital eccentricity/periapse, but typically this only occurs close to plunge. The other problem at high mass ratio is the break down of the perturbative approach – the expressions (13–15) are based on a fit to calculations that have been carried out to leading order in the mass ratio. As the mass ratio become moderate, this is no longer sufficiently accurate. Broadly speaking, our results should apply to mass ratios less than $\sim 10^{-2} - 10^{-1}$.

The results in this paper apply to orbits in the Schwarzschild spacetime, while theoretical models (Volonteri et al. 2005) and some observational evidence (Miniutti et al. 2004; Fabian et al. 2005) indicate that most astrophysical black holes will have significant spins. While some perturbative results are available that compute the radiation from orbits around spinning black holes (Poisson 2004), there is not yet sufficiently generic data available from state of the art computations to fit for that situation. However, the arguments that led to the construction of the fitting function that performs so well in this case also apply when the central black hole has spin. Once a sufficient quantity of data is available, it should be possible to construct a fit of similar form, although it will be more complicated as the fit will depend on three parameters – the black hole spin, the radius of the periapse and the inclination of the orbit. For more generic applicability, eccentricity can also be included as a fourth parameter, though again this can only be done once perturbative calculations for generic orbits have been completed.

We thank Marc Freitag for useful discussions and comments on the manuscript. SLL and JRG thank the Aspen Centre for Physics for hospitality while the manuscript was being finished. This work was supported in part by NASA grants NAG5-12834 (JRG, DJK) and NAG5-10707 (JRG) and by St.Catharine’s College, Cambridge (JRG). SLL acknowledges support at Penn State from the Center for Gravitational Wave Physics, funded by the NSF under cooperative agreement PHY 01-14375, as well as support from Caltech under LISA contract number PO 1217163.

REFERENCES

- Barack, L. and Cutler, C., 2004, *Phys. Rev. D*, 69, 082005
- Cutler, C., Kennefick, D. & Poisson, E. 1994, *Phys. Rev. D*, 50, 3816.
- Fabian, A. C., Miniutti, G., Iwasawa, K. and Ross, R. R., 2005, *MNRAS*, 361, 795

- Freitag, M., 2001, *Class. Quantum Grav.*, 18, 4033
- Freitag, M., 2003, *ApJ*, 583, L21
- Freitag, M. & Benz, W., 2002, *A&A*, 394, 345
- Gair, J. R., Barack, L., Creighton, T., Cutler, C., Larson, S. L., Phinney, E. S. and Vallisneri, M., 2004, *Class. Quantum Grav.*, 21, S1595
- Gair, J. R. and Glampedakis, K., 2005, preprint gr-qc/0510129
- Gair, J., Kennefick, D. & Larson, S., 2005, *Phys. Rev. D*, **72**, 084009
- Goodman, J. and Tan, J. C., 2003, *ApJ*, 608, 108
- Hils, D. and Bender, P. L., 1995, *ApJ Lett.*, 445, L7
- Hopman, C. and Alexander, T., 2005, *ApJ*, 629, 362
- Ivanov, P. B., 2002, *MNRAS*, 336, 373
- Levin, Y., 2003, preprint astro-ph/0307084
- Martel, K., 2004, *Phys. Rev. D*, 69, 044025
- Miller, M. C., Freitag, M., Hamilton, D. P. and Lauburg, V. M., 2005, *ApJ Lett.*, 631, L117
- Miniutti, G., Fabian, A. C. and Miller, J., 2005, *MNRAS*, 351, 466
- Peters, P. C., 1964, *Phys. Rev.*, **136**, 4B 1224
- Peters, P. C. & Mathews, J., 1963, *Phys. Rev.*, **131**, 435
- Poisson, E., “The Motion of Point Particles in Curved Spacetime”, *Living Rev. Relativity* 7, (2004), 6. [Online article]: cited on 17/6/2005, <http://www.livingreviews.org/lrr-2004-6>
- Ruffini, R. & Sasaki, M., 1981, *Prog. Theor. Phys.*, 66, 1627
- Sigurdsson, S. & Rees, M., 1997, *MNRAS*, 284, 318
- Volonteri, M., Madau, P., Quartet, E. and Rees, M., 2005, *ApJ*, 620, 69